

Article

Catalytic Hydrothermal Liquefaction of *Brachychiton populneus* Biomass for the Production of High-Value Bio-Crude

Ikram Eladnani ¹, Maria Paola Bracciale ^{2,*} , Martina Damizia ^{2,*} , Seyedmohammad Mousavi ² , Paolo De Filippis ² , Rajae Lakhmiri ¹ and Benedetta de Caprariis ²

¹ Laboratory of Chemical Engineering and Valorization of the Resources, Faculty of Sciences and Techniques of Tangier, Abdelmalek Essaâdi University, Km 10 Road of Ziaten, P.O. Box 416, Tangier 93000, Morocco

² Department of Chemical Engineering Materials Environment, SAPIENZA University of Rome, Via Eudossiana 18, 00184 Rome, Italy

* Correspondence: mariapaola.bracciale@uniroma1.it (M.P.B.); martina.damizia@uniroma1.it (M.D.)

Abstract: The current study focused on the heterogenous catalytic hydrothermal liquefaction (HTL) of *Brachychiton populneus* biomass seed, using Ni as hydrogenation catalyst and Fe as active hydrogen producer. The activity of Ni metal and of Ni/Al₂O₃ in the HTL of seed (BS) and of a mixture of seed and shell (BM) was studied. To establish the best operating process conditions, the influence of variation of temperature and reaction time on the product yields was also examined. The highest bio-crude yields of 57.18% and 48.23% for BS and BM, respectively, were obtained at 330 °C and 10 min of reaction time, in the presence of Ni/Al₂O₃ as catalyst and Fe as hydrogen donor. Elemental analysis results showed that at these operative conditions, an increase of the higher heating value (HHV) from 25.14 MJ/kg to 38.04 MJ/kg and from 17.71 MJ/kg to 31.72 MJ/kg was obtained for BS and BM biomass, respectively, when the combination of Fe and Ni/Al₂O₃ was used. Gas chromatography–mass spectrometry (GC-MS) and Fourier transform infrared spectroscopy (FT-IR), used to determine the oils' chemical compositions, showed that the combined presence of Fe and Ni/Al₂O₃ favored the hydrodeoxygenation of the fatty acids into hydrocarbons, indeed their amount increased to ≈20% for both biomasses used. These results demonstrate that the obtained bio-crude has the capacity to be a source of synthetic fuels and chemical feedstock.

Keywords: hydrothermal liquefaction; *Brachychiton populneus*; catalytic HTL; energy recovery



Citation: Eladnani, I.; Bracciale, M.P.; Damizia, M.; Mousavi, S.; De Filippis, P.; Lakhmiri, R.; de Caprariis, B.

Catalytic Hydrothermal Liquefaction of *Brachychiton populneus* Biomass for the Production of High-Value Bio-Crude. *Processes* **2023**, *11*, 324. <https://doi.org/10.3390/pr11020324>

Academic Editor: Alok Kumar Patel

Received: 15 December 2022

Revised: 9 January 2023

Accepted: 16 January 2023

Published: 19 January 2023



Copyright: © 2023 by the authors. Licensee MDPI, Basel, Switzerland. This article is an open access article distributed under the terms and conditions of the Creative Commons Attribution (CC BY) license (<https://creativecommons.org/licenses/by/4.0/>).

1. Introduction

The increase in the energy demand and the limitation on the emission of CO₂ imposed by most governments make the replacement of the fossil fuels with more sustainable sources urgent [1]. In this context, biofuels obtained from biomass have been selected as one of the possible alternatives. Residual biomass, such as forestry and agricultural residues, and organic waste, such as sewage sludge, are gaining interest worldwide due to their wide availability and non-competitiveness with arable lands. The conversion of biomass into biofuels can be performed with many different biochemical and thermochemical technologies: anaerobic digestion, combustion, pyrolysis, gasification, hydrothermal liquefaction, etc. Among them, hydrothermal liquefaction (HTL) is one of the most effective technologies, able to efficiently convert several biomass types, such as rice straw [2], peanut shell [3], oak wood [4] sugar beet pulp [5] and microalga [6,7], into more valuable liquid bio-crude. Furthermore, the process is carried out at a medium temperature (250–400 °C) and under high pressure (5–20 MPa), using water as a solvent [8]. The influence of several process variables, such as temperature [9], residence time [10], catalyst activity [11] and water-biomass ratio [12], on the product yields has been widely investigated in literature in order to find the optimal conditions. Generally, during HTL, wet biomass reacts with water, producing numerous compounds that are mainly distributed into four phases: a liquid bio-crude, an aqueous phase rich in organic soluble compounds, a gas phase and a solid residue. The

bio-crude produced via HTL generally contains lower oxygen content with respect to the bio-crude obtained by the traditional pyrolysis process [13] and, therefore, it possesses higher heating value (HHV) (in the range of 30–36 MJ/kg in HTL and 22–28 MJ/kg for pyrolysis). However, the still-high oxygen concentration of the HTL bio-crude (in the range of 10–20%) makes it chemically unstable and, therefore, not ready for direct use. Expensive upgrading processes that require high amounts of H₂ are, therefore, needed to make it ready for commercialization [14]. For these reasons, the direct production of a high-quality bio-crude is fundamental to decrease the intensity of the up-grading process and to make the overall process more sustainable.

The use of catalysts in HTL can be an effective solution to partially up-grade the bio-crude during its production. Numerous studies demonstrated the key role played by the catalyst in increasing oil yield and enhancing oil quality [15]. Various catalysts type, both homogeneous and heterogeneous in nature, such as organic acids (formic acid, acetic acid), alkaline materials (potassium hydroxide), salts and zero-metals, have been successfully used in the HTL process [16]. Based on literature results, the use of homogeneous catalysts makes it possible to obtain high bio-crude yields without a significant improvement of its quality. Furthermore, they cannot be separated from the aqueous phase recovered, making them responsible for the expensive wastewater treatments needed before the discharge.

The use of heterogeneous catalysts solves this issue; they can be easily recovered and recycled at the end of the reaction. Furthermore, several studies have highlighted their ability to enhance both bio-crude yields and quality [17,18]. In particular, nickel metal (Ni) is a well-known hydrogenation catalyst, and in the authors' previous work, the use of supported Ni coupled with Fe as the hydrogen producer enhanced the biomass conversion into high-quality bio-crude [19]. The results showed that the highest bio-crude yields reached were 26.5% and 24.9% for Fe and Ni, respectively. The heterogeneous catalyst performances were significantly affected by the type of support selected and by the synthesis method used, with the parameters significantly affecting the catalyst's morphology and, therefore, the accessibility to the Ni active sites [11].

The Ni-Co/activated carbon was employed as a catalyst to enhance the hydrothermal liquefaction of alkali lignin, with a maximum bio-oil yield of 72% achieved at 280 °C using ethanol as solvent [20]. Additionally, Halil Durak et al. investigated the HTL of *Lactuca scariola*, employing Fe as catalyst and obtaining an oil yield of 16.93% [21]. The catalytic HTL of woody biomass employing Fe + Na₂CO₃ as catalyst was reported by Zhao et al. [22]. The maximum bio-crude yield was 81%. The effect of mesoporous Ni-Al/SBA-15 catalyst on hydrothermal liquefaction of rice straw was deeply studied by Yong-Jie Ding et al., obtaining a maximum oil yield of 44.3% [23]. Saber et al. [24] used Ni/SiO₂ in the catalytic HTL of microalgae biomass, achieving a maximum bio-oil yield of 30%.

Among the biomass types that can be exploited for the production of bio-fuels, lipid-containing sources are recognized as the most valuable due to the similarity of lipid structures to petroleum-based diesel fuels [25,26]. Generally, biodiesel is obtained from lipids through transesterification processes, converting triacyl-glycerides (TAGs) into fatty acid methyl esters (FAMES). However, conventional transesterification processes require the use of high-quality TAG feedstocks, such as vegetable oils, and large amounts of alcohol as solvents [27]. An interesting alternative for the production of biofuels is the direct conversion of waste biomass rich in lipids by HTL, followed by an expensive up-grading step, such as catalytic hydrodeoxygenation (HDO), which requires large amounts of hydrogen [28]. Direct feedstock conversion in hydrothermal environments (e.g., 250–350 °C, 4–16 MPa) eliminates the need for lipid extraction, converting the whole biomass into bio-crude, minimizing net energy required. The use of hydrogenation catalysts, such as bimetallic catalysts, has proven effective in catalyzing the hydrogenation, decarboxylation/decarbonylation and deoxygenation of the FFAs and in promoting in situ generation of H₂ via an aqueous phase reforming directly in the HTL reactor, producing a partially up-graded bio-crude and, thus, minimizing the impact of the up-grading step on the whole process economy [29–31].

Brachychiton populneus is a popular decoration plant cultivated mainly in Australia and North Africa. Its fruits contain non-edible seed oils that are considered potential feedstock for biodiesel synthesis. The extraction of lipids from *Brachychiton populneus* seeds (BS) to produce bio-diesel was investigated only by Dawood et al., who produced bio-diesel from *Brachychiton populneus* seed oil using heterogenous green NiO as a nanocatalyst. The biodiesel yield was of 97.5% under optimized transesterification conditions (1:9 oil to methanol molar ratio and 2.5% of nanocatalyst at 85 °C) [32].

The aim of this study was to produce bio-crude from HTL of *Brachychiton populneus* seed by valorizing all the biomass components, producing linear hydrocarbons from lipids and aromatic compounds from the other biomass components, such as lignin and cellulose. In this way, the bio-crude would be a perfect raw material for the production of sustainable aviation fuel. The use of Ni-based catalysts coupled with metallic Fe has been investigated to produce a partially up-graded bio-crude.

Specifically, *Brachychiton populneus* seed (BS) and a mixture of seed and shell (BM) were selected as feedstock for the HTL process. The investigation was focused on the optimization of the process conditions: liquefaction temperature, retention time and catalyst effect. The bio-crude was characterized by elemental analysis (C, H, N, O, S), gas chromatography–mass spectrometry (GC-MS) and Fourier transform infrared spectroscopy (FT-IR).

2. Materials and Methods

2.1. Materials

The fruits of *Brachychiton populneus* were collected in May in the city of Tangier, in the northern region of Morocco. The harvested fruits were separated from their leaves and branches, and the seeds (BS) were separated from the shell. They were then washed with deionized water and dried in the oven at 60 °C for 72 h. After drying, the seeds were then crushed in a grinder to obtain a powder (150 < dp < 300 µm). The composition of the BS and its mixture with shell (BM) is presented in Table 1.

Table 1. Proximate and elemental analysis of BS and BM raw materials.

	BS	BM
Proximate analysis (wt%)¹		
Moisture (%)	7.3	7.5
Volatile (%)	72.3	79.2
Fixed carbon (%)	16.5	9.8
Ash (%)	3.9	3.5
Elemental analysis (wt%)²		
C	56.75	45.42
H	7.41	6.08
N	1.91	2.10
O ³	31.06	46.40
Protein ⁴	10.5	11.6
H/C (molar ratio)	1.57	1.60
HHV (MJ/kg)	25.14	17.71

¹ Dry basis; ² dry ash free; ³ calculated by difference; ⁴ estimated by nitrogen-to-protein conversion factor of 5.5 [33].

The Ni and Fe powders (assay > 97% and 20 < dp < 50 µm) and acetone, used for the bio-crude extraction, were obtained from Sigma-Aldrich company. Aluminum oxide powder (Al₂O₃) was supplied by Sigma-Aldrich (assay > 99.99% and 150 < dp < 300 µm).

2.2. Methods

The effects of various parameters, such as temperature (240, 270, 300, 330 °C), residence time (10, 30, 60, 120, 180 min) and type of Ni-based catalyst used (10 wt% of the biomass weight), were studied. In the tests with the hydrogen donor, the amount of Fe added was

equal to 50 wt% of the biomass weight. Each experiment was performed in a stainless steel tubular micro-reactor (length 120 mm and inner diameter of 15 mm) using 1 g of dried biomass and 5 g of distilled water mixed together and, in catalytic tests, 0.1 g of catalyst. The reactor, connected to a mechanical stirrer, was heated in a fluidized sand bath (average heating rate: $60\text{ }^{\circ}\text{C}\cdot\text{min}^{-1}$) at the desired temperature and maintained in isothermal conditions for the selected reaction time. The residual air inside the reactor was removed via purging with a nitrogen flow. The pressure in the reactor was autogenerated, ranging between 7 and 15 MPa. At the end of the tests, the reactor was quenched in a water bath and weighted. Then, the reactor was opened to remove the gaseous products and weighted again to determine the amount of gas phase produced. The water phase was discharged via filtration and the bio-crude was extracted from the solid residue by using 50 mL of acetone as solvent in a Soxhlet extractor. The oil phase was recovered from the extracted solution by evaporating the acetone at $60\text{ }^{\circ}\text{C}$ and 556 mbar using a rotary evaporator. Finally, the reactor was placed in an oven at $80\text{ }^{\circ}\text{C}$ for 24 h to dry the char. All the tests were performed in triplicate to confirm the repeatability of the results; the values reported in this study are the mean values [34].

The Ni/ Al_2O_3 catalyst was synthesized according to the procedures reported in the authors' previous work [35]. Briefly, 5 wt% of Ni loading on Al_2O_3 support was obtained via the wet-impregnation method, using nickel nitrate water solution ($\text{Ni}(\text{NO}_3)_2\cdot 6\text{H}_2\text{O}$, Sigma-Aldrich company). After the impregnation, the water was evaporated at $80\text{ }^{\circ}\text{C}$ and the catalyst precursor was calcined at $550\text{ }^{\circ}\text{C}$ for 4 h in air atmosphere. XRD diffractogram of the metal-supported Al_2O_3 catalyst is displayed in Figure 1. Diffraction peaks corresponding to γ -alumina are clearly visible at 25.54° , 35.12° , 37.76° , 43.34° , 52.52° , 57.46° , 66.48° and 68.16° , along with those at $2\theta = 37.32^{\circ}$, 63.0° , 75.58 and 79.58° assigned to the cubic phase of nickel oxide. Before use, Ni/ Al_2O_3 was reduced in a tubular reactor at 300°C in 10 vol% of H_2 stream diluted in argon for 2 h.

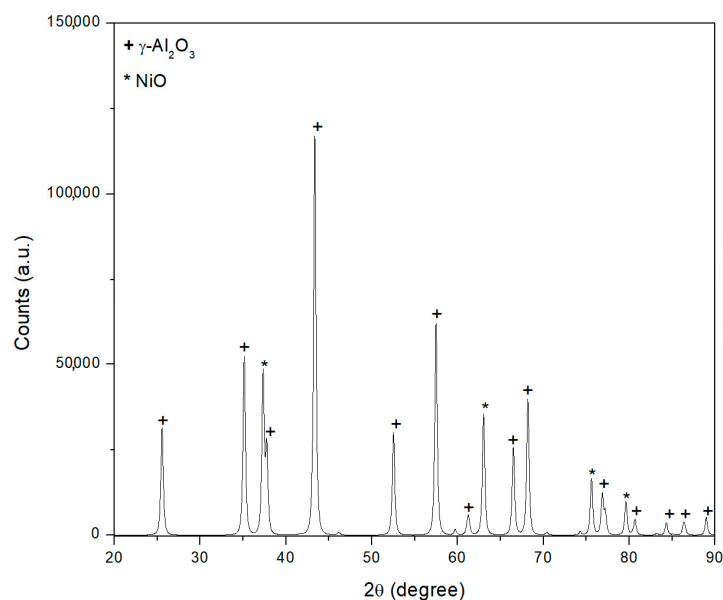


Figure 1. XRD diffractogram of synthesized Ni/ Al_2O_3 catalyst.

2.3. Characterization

Proximate analysis for determination of moisture, volatile matter, fixed carbon and ash contents in biomass was performed with a thermogravimetric methodology [36], using a SDT Q600 thermal analyzer (TA Instruments; New Castle, DE, USA). All analyses were conducted in two steps: (1) moisture and volatiles determination under nitrogen (N_2) at a flow rate of $130\text{ mL}\cdot\text{min}^{-1}$; (2) fixed carbon and ash contents were determined under air at a flow rate of $100\text{ mL}\cdot\text{min}^{-1}$. For moisture (M) content determination, heating at $110\text{ }^{\circ}\text{C}$ was employed until a constant weight was reached. Volatile matter (VM) was determined

as weight loss due to heating to $T \approx 600$ °C and ash (A) is the residual inorganic matter determined after combustion under dry air. Subsequently, the percentage of fixed carbon (FC) was calculated by the difference between M, VM and A. To avoid limitations on mass and heat transfer, about 10 mg of sample and uncovered platinum crucibles were used.

The compositions of the feedstock and bio-crude (C, H, N, S and O) were determined using an Eurovector EA3000 elemental analyzer. C, H, N, S and O represent the wt% of each atom in the samples. At minimum, triplicate analyses were conducted for each sample; the mean values were used in the Dulong's formula (Equation (1)) to calculate the higher heating values (HHV) of each sample:

$$\text{HHV (MJ/kg)} = 0.338 C + 1.428 \left(H - \frac{O}{8} \right) + 0.095 S \quad (1)$$

The energy recovery (E.R.) was calculated using the following equation:

$$\text{E.R. (\%)} = \frac{\text{HHV}_{\text{biocrude}} \times \text{Yield}_{\text{biocrude}}}{\text{HHV}_{\text{dry feedstock}}} \times 100 \quad (2)$$

The chemical composition of bio-crudes was detected by gas chromatography–mass spectrometry (GC-MS). GC analysis was performed using a 6890 model gas chromatograph with helium as carrier gas and a mass spectroscopy detector (Agilent), using a thin-film (30 m × 0.32 mm, 0.5 µm film thickness) HP-MS5 capillary column supplied from HP.

Fourier transform infrared (FT-IR) spectroscopy was used to investigate the functional groups of bio-crude. Infrared measurements were carried out with a Bruker Vertex 70 spectrometer (Bruker Optik GmbH) equipped with a single reflection Diamond ATR cell. Spectra were recorded with a 3 cm⁻¹ spectral resolution in the mid infrared range (400–4000 cm⁻¹) using 512 scans.

3. Results and Discussion

3.1. Liquefaction Yields

3.1.1. Effect of Temperature

Temperature is a key parameter in the HTL that affects both bio-crude yields and quality [37]. The effect of temperature on the product distribution in the HTL of *Brachy-chiton populneus* seed (BS) and of the mixture of seed and shell (BM) was studied, varying the reaction temperature from 240 °C to 330 °C. In authors' previous work, 330 °C was demonstrated to be the optimal temperature to maximize the oil yields in lignocellulosic biomass [4]. Furthermore, from literature, it is known that the optimal range for lipid production in HTL is 280 ± 40 °C in order to avoid cracking reactions at higher temperatures [16]. All tests were performed at constant reaction time of 60 min. Figure 2 shows the yields of the products obtained (gas, bio-crude, char and water soluble) at each temperature tested. The trend of the bio-crude yields confirms that the increase of temperature favors the biomass conversion into bio-crude rather than into char and gases [16,38,39]. The highest bio-crude yields obtained in the tested range of temperature of 40.50% and 31.21% for BS and BM, respectively, were obtained at 330 °C. The char yields followed the opposite trend, achieving the maximum value of 19% and 28% for the BS and BM, respectively, at the lowest temperature tested (240 °C). The minimum values for the char yields, equal to 9% and 16% for BS and BM, respectively, were produced at the highest temperature (330 °C) tested. The amount of water-soluble compounds decreased with increasing temperature due to the promotion of recombination reactions to form compounds that were higher molecular weight, which were no longer soluble in water and, thus, they migrated into the bio-crude phase. These results demonstrated that, as expected, the amounts of bio-crude produced from seed alone (BS) were always higher than those obtained with BM because of the higher lipids concentration in the BS with respect to the mixture of seed and shell; the presence of shell in the BM feedstock introduces lignin in the reactive environment, which favors the char formation at the expense of bio-crude yields.

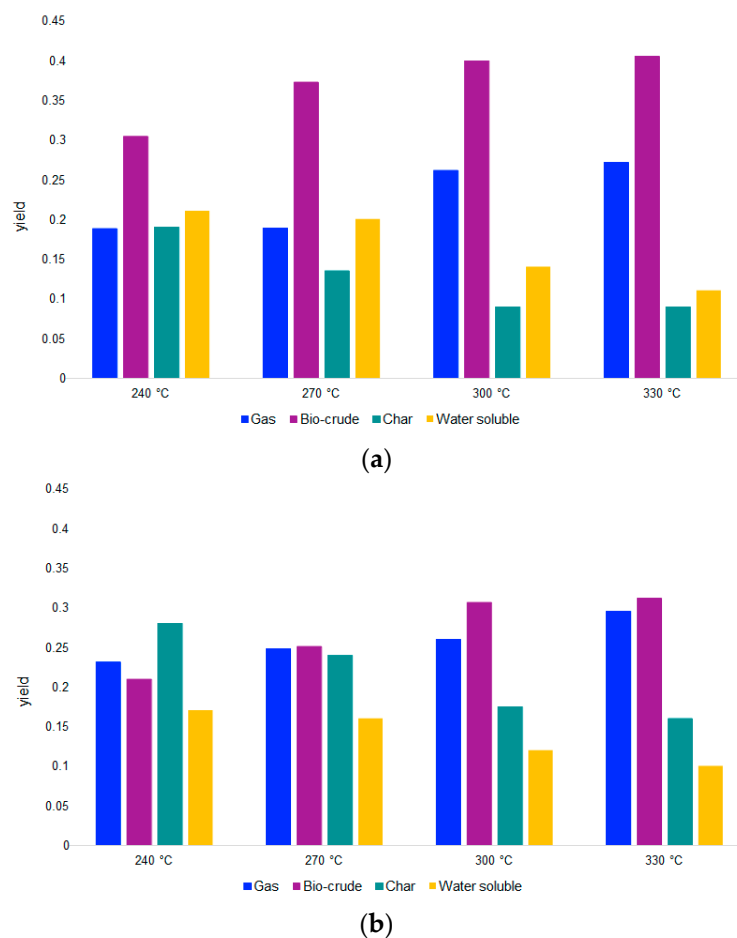


Figure 2. Effect of temperature on the products distribution in HTL of (a) BS and (b) BM. The tests were performed at a constant reaction time of 60 min.

All the further tests reported in this study were thus performed at 330 °C, which was considered to be the optimal reaction temperature among the range tested for the chosen system.

3.1.2. Effect of Reaction Time

The reaction time also played a fundamental role in the bio-crude production. Firstly, the biomass decomposed into many fragments, which can effect one of two competitive pathways: (1) further decomposition to produce more bio-crude and gases or (2) fragment re-polymerization to give char [40]. Longer reaction times usually promote the char formation through re-polymerization reactions.

The influence of reaction time on the product distribution were studied by performing HTL tests at 10, 30, 60, 120 and 180 min, constantly maintaining the temperature at the optimal value (330 °C) determined in the previous section. The obtained results are presented in Figure 3. It has been noticed that with the increase of reaction time, the bio-crude yield decreased [41]. The longer reaction times, in fact, favored condensation and repolymerization reactions, which contributed to the increase of the gas phase and to the decrease of both the oily and the water-soluble organic compound yields.

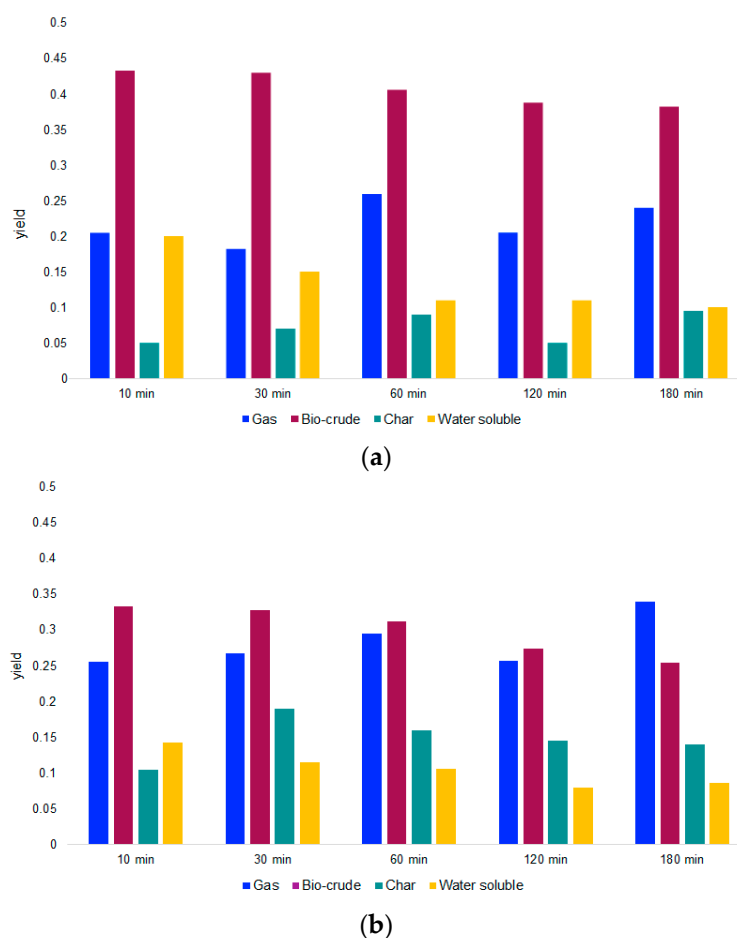


Figure 3. Effect of the reaction time on the product distribution with (a) BS and (b) BM at 330 °C.

The results of BS and BM confirmed the trend—varying the reaction time from 10 min to 180 min led to a decrease of bio-crude yields from 43.17% to 38.11% in the case of BS and from 33.29% to 25.45% with BM. Therefore, the optimal reaction time that maximized the bio-crude yields for both BS and BM was determined to be equal to 10 min. These results are in accordance with the literature. Li et al. [42] found that in the first 15 min the bio-crude yield increased and, subsequently, by increasing the retention time, this tended to decrease due to re-polymerization and condensation reactions. Furthermore, Sugano et al. [43] noted a decrease in bio-oil yield for long residence times and concluded that faster residence times resulted in higher yields.

Operating a reactor system with a lower retention time is favorable, not only because the bio-crude production rate will be higher, but also the heat loss per unit mass of bio-crude produced can be significantly reduced, making the process more energy efficient.

3.1.3. Effect of Ni-Based Catalysts Addition with and without Fe as Hydrogen Producer

The hydrogenation activity of Ni and Ni/Al₂O₃ on the HTL of BS and BM was studied at the optimal operative conditions previously determined (330 °C for 10 min), adding 10 wt% of catalyst in the reactor. A test with 50 wt% of Fe metal, with respect to the biomass weight, was also performed in order to supply the gaseous hydrogen needed to maximize the catalyst hydrogenation activity via the oxidation of Fe with water in subcritical conditions. In a previous work, the feasibility of producing gaseous H₂ via the oxidation of Fe with water in HTL conditions, at the same temperature range of this work, was demonstrated [4]. The results obtained are summarized in Figure 4. The results of the test adding only Fe (with no Ni-based catalyst) are also reported to take into account the

positive influence of the presence of active gaseous hydrogen on the bio-crude yield and quality. The product distribution of the blank test is also reported.

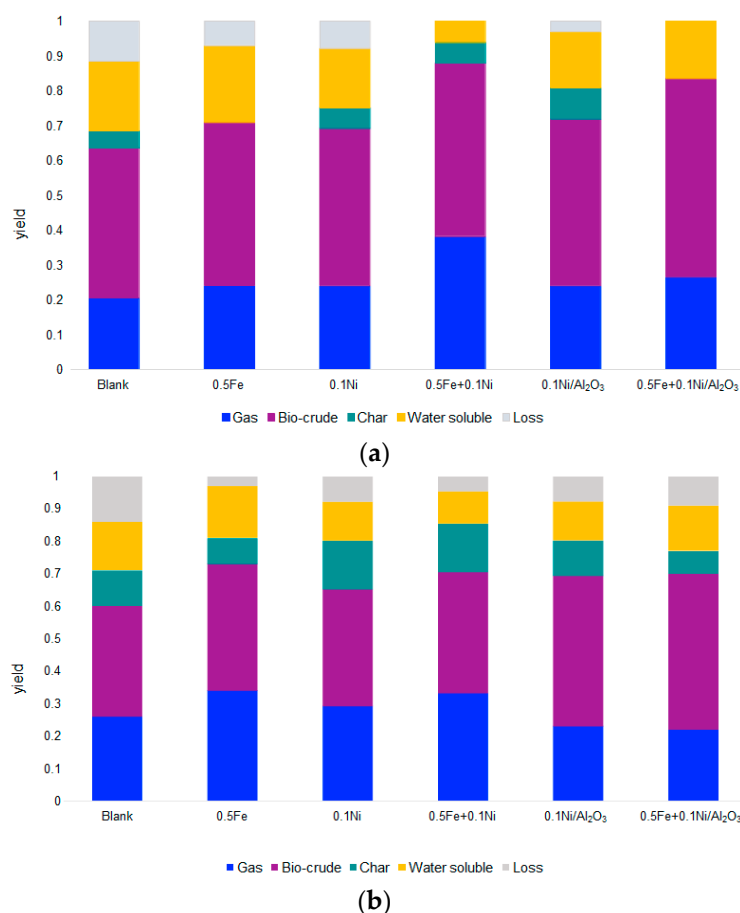


Figure 4. Effect of catalyst in HTL of (a) BS and (b) BM at 330 °C for a residence time of 10 min.

The results suggest that the use of both Ni metal and Ni supported on Al₂O₃ determines an increase in the bio-crude yields. The catalytic activity of Ni in the hydrodeoxygenation of the bio-crude molecules is evident given that the bio-crude yields increased for both BS and BM. Fe seemed to produce only a slight effect on the increase of the oil yields when added alone—the bio-crude yield was not considerably improved, while an increase of the water soluble compounds was always obtained. As already proved in the authors' previous work [19], Fe can act as an active hydrogen producer in the reaction environment—the H₂, in the absence of a hydrodeoxygenation catalyst, reacts with the unstable bio-crude molecules stabilizing them and forming low-molecular-weight oxygenated compounds that are soluble in the water phase. The use of a dispersed form of Ni, such as in Ni/Al₂O₃ catalyst, can improve considerably the bio-crude yields and its action becomes even more evident when this catalyst is used in combination with Fe. Looking at the results, it is clear that there was a synergistic effect between the two materials, which allowed us to obtain 57% and 48% of bio-crude yields in the case of BS and BM, respectively.

The combined presence of Fe and Ni/Al₂O₃ allowed for the exploitation of the hydrodeoxygenation activity of the Ni enhanced by the presence of active H₂ in the reactor.

3.2. Characterization of Products

3.2.1. Feedstock and Bio-Crude Elemental Analysis

The elemental composition and higher heating value (HHV) of the feedstocks and bio-crudes obtained from the HTL of *Brachyichiton* seed (BS) and mix (BM) in the optimum condition (330 °C and 10 min) were determined to assess the quality of the produced

bio-crude. Looking at Table 2, the combination of the Fe and Ni/Al₂O₃ catalyst led to an oil having the highest carbon content (77.15% for BS and 71.02% for BM), higher H content and, therefore, the lowest O amount. These results indicate that the Ni-based catalyst promotes the deoxygenation and/or decarbonylation reactions.

Table 2. Elemental analysis of BS and BM raw material and bio-crudes obtained at 330 °C for a residence time of 10 min.

	C	H	N	O ¹	H/C ²	E. R. (%)	HHV (MJ/kg)
BS—Blank	65.45	8.67	1.63	24.25	1.58	52.73	30.68
BS—0.5Fe	76.54	9.71	1.76	11.99	1.52	86.95	37.30
BS—0.5Fe-0.1Ni	70.47	8.70	1.82	19.21	1.44	65.42	33.02
BS—0.5Fe-0.1Ni/Al ₂ O ₃	77.15	10.03	2.10	10.72	1.56	86.56	38.04
BM—Blank	62.78	6.71	1.03	29.48	1.28	50.06	26.62
BM—0.5Fe	69.48	7.68	0.91	21.93	1.32	64.11	31.11
BM—0.5 Fe + 0.1 Ni	68.23	7.57	0.90	23.30	1.33	63.80	30.38
BM—0.5Fe-0.1Ni/Al ₂ O ₃	71.02	7.79	1.10	22.29	1.31	86.31	31.72

¹ Calculated by difference; ² molar ratio.

The HHV of bio-crudes was greater in the presence of Ni coupled with Fe; using the couple Fe + Ni/Al₂O₃, the HHV value rose to 38.58 and 31.24 MJ/kg, while raw biomass had an HHV of 6.88 and 16.87 MJ/kg for BS and BM, respectively. Additionally, the presence of the catalyst enhanced the energy recovery (E.R.) values, favoring a high-quality bio-crude formation.

More details on the chemical composition of the bio-oils obtained from the GC-MS analysis and FT-IR spectroscopy are presented in the following paragraphs.

3.2.2. GS-MS of Bio-Crude

The chemical composition of the HTL oil was characterized by GC-MS analysis. As reported in Figure 5, the blank oils were mainly composed by fatty acids, which accounted for 80% in the case of BS and 70% in the case of BM. This result was expected, given that the BS had a higher amount of lipids (25% of the dried biomass), which were hydrolyzed to form fatty acids, one of the main components of the produced bio-crude. The main fatty acids were hexadecenoic (about 25% of the total) and octadecanoic (about 70% of the total). In the oil obtained from the seed (BS), the other major compounds were amides that were produced via the degradation of the phospholipids and proteins. The oil from the mix (BM) also contained a considerable percentage of phenols (up to 33% for the test with Ni) produced by the decomposition of the lignin, which was a component of the seed shell. When catalysts were used, the composition of the oil changed; the presence of Ni favored the hydrodeoxygenation of the fatty acids into hydrocarbons. In fact, when 50 wt% Fe – 10 wt% Ni and 50 wt% Fe + 10 wt% Ni/Al₂O₃ were added, their percentage area increased to 19% and 20%, respectively, for the BS and to 22.61% and 20.30% for the BM at the expense of the fatty acids. The hydrocarbon components for the tests made with 50 wt% Fe + 10 wt% Ni/Al₂O₃ are reported in Table 3 on the basis of their percentage area.

According to the literature, in the initial stage, the bio-macromolecules, such as carbohydrates (hemicellulose, cellulose, polysaccharides), lipids (triglycerides) and proteins, were hydrolyzed with water to form their corresponding monomer products and small molecular compounds, including oligo- and monosaccharides (glucose, cellobiose and xylose), aliphatic acids (FFAs) and amino acids, respectively. As reported in a previous work by the authors [44], the monosaccharides could degrade by two competitive pathways: (1) dehydration to furan derivatives (furfural, 5-hydroxymethylfurfural and 5-methylfurfural) and (2) retro-aldol reaction to C₂–C₄ ketones and carboxylic acids (3-hydroxy-2-butanone, acetic acid and propionic acid). Thanks to the presence of active hydrogen generated by the Fe–water redox reaction and to the action of the Ni hydrogenation catalyst, the furan derivatives could then be hydrogenated to 2-cyclopenten-1-ones.

Furthermore, the Fe_3O_4 formed could function as a base catalyst accelerating the retro-aldol reaction. The scheme of bio-crude production in the presence of Fe and Ni is reported in authors' previous work for the lignocellulosic biomass [44].

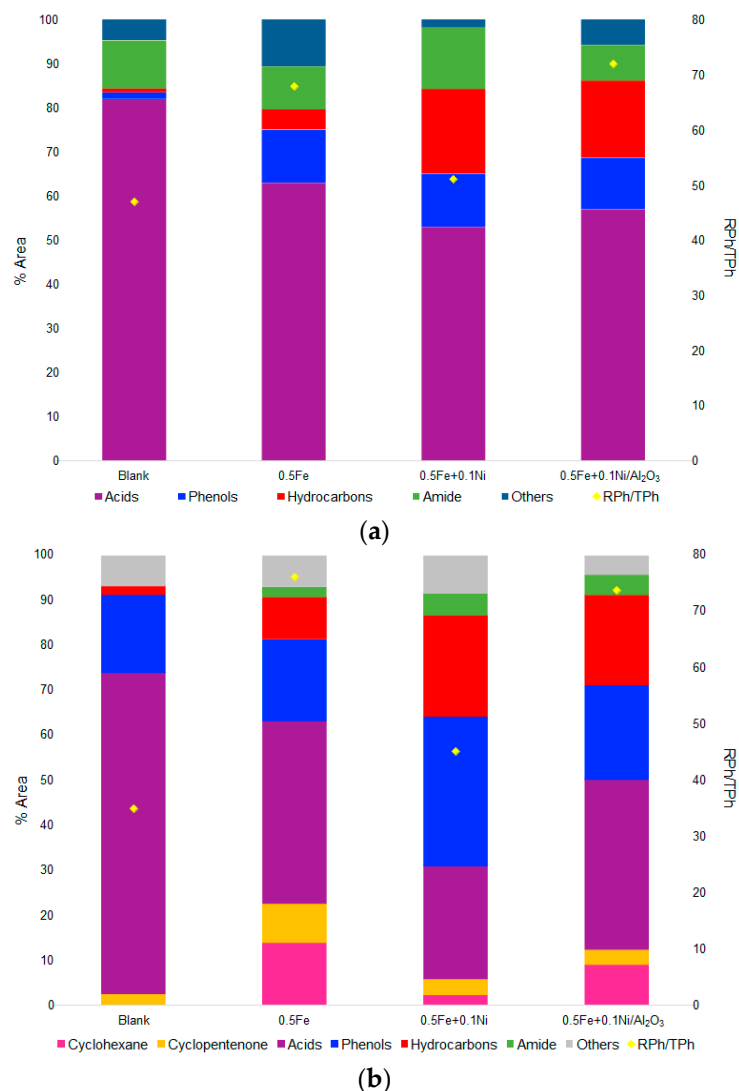


Figure 5. Compounds identified by GC-MS in the bio-crude at 330 °C, for a residence time of 10 min, for (a) BS and (b) BM. RPh/TPH: ratio of reductive phenols to the total phenols.

Table 3. Composition (% area) of the hydrocarbons in the bio-crude obtained with 0.5Fe + 0.1Ni/Al₂O₃ at 330 °C and for a residence time of 10 min.

	BS	BM
1-Tetradecene	0.56	-
Tetradecane	0.97	2.44
Pentadecane	2.53	4.55
1-Hexadecene	1.92	-
Hexadecane	1.01	2.72
8-Heptadecene	0.84	-
Heptadecane	12.17	10.59

Triglycerides hydrolyze to produce glycerol and a mixture of saturated (octadecanoic acid) and unsaturated fatty acids (hexadecenoic acid). The latter can be subsequently hydrogenated to form saturated ones (by breaking π bonds) using in situ active hydrogen pro-

duced by the Fe particles and by the aqueous phase reforming of glycerol (Figure 6) [26,45]. Saturated FFAs can undergo deoxygenation following three different Ni-catalyzed reactions: (1) decarboxylation: loss of a CO_2 molecule to form heptadecane ($\text{C}_{17}\text{H}_{36}$); (2) decarbonylation: elimination of CO and H_2O to form long-chained hydrocarbons (C_{14} , C_{15} , C_{16} , C_{17}), such as heptadecene ($\text{C}_{17}\text{H}_{34}$); (3) heptadecene can, in turn, be hydrogenated to heptadecane. The stearyl alcohol intermediate can also undergo decarbonylation to heptadecane [31].

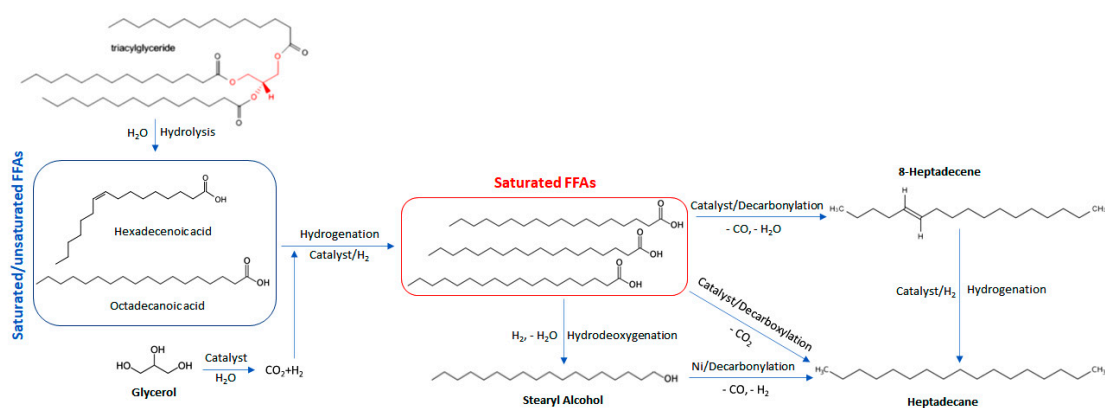


Figure 6. HTL conversion pathway of triacylglycerides to linear alkanes in the presence of Fe-Ni/ Al_2O_3 catalyst.

The hydrothermal process of lignin generates significant quantities of solid residue. However, it has been demonstrated that the presence of Fe ensures active hydrogen generation during lignin depolymerization, significantly suppressing the repolymerization of lignin-derived compounds [44]. Lignin is hydrolyzed to phenolic oligomers and monomers, which can also decompose more through strong hydrogenation on the benzene ring structure. The catalysts also have a strong effect on the phenolic compounds. The aromatic compounds are classified into reduced aromatics (phenolic compounds bearing an alkyl chain: methyl-, ethyl- and propyl phenol derivatives, plus phenol, guaiacol, syringol and hydroquinone) and oxygenated aromatics, which are unsaturated and oxygenated phenols (phenolic compounds bearing alkene side chain such as eugenol and isoeugenol). The ratio of reductive phenols (RPh) to the total phenols (TPh) is an important index for the hydrogenation effect [46]. The amount of RPh increases considerably when H_2 is present in the system due to the oxidation of metallic Fe, as confirmed by the higher hydrogen content in the elemental analysis results—the RPh/TPh ratio increased for both samples from approximately 45% to 70%. In the case of BM, the presence of almost 10% cyclohexane confirmed the strong hydrodeoxygenation activity as a result of the addition of Fe and Ni/ Al_2O_3 .

3.2.3. Infrared Analysis of Bio-Crudes

FT-IR was used to detect the functional groups in the BM bio-crudes obtained at 330°C and for a residence time of 10 min. As shown in Figure 7, the FT-IR spectra are quite similar, with absorption bands indicating the presence of aromatic hydrocarbons and phenols, as well as oxygen-containing compounds (esters, ketones, aldehydes and alcohols).

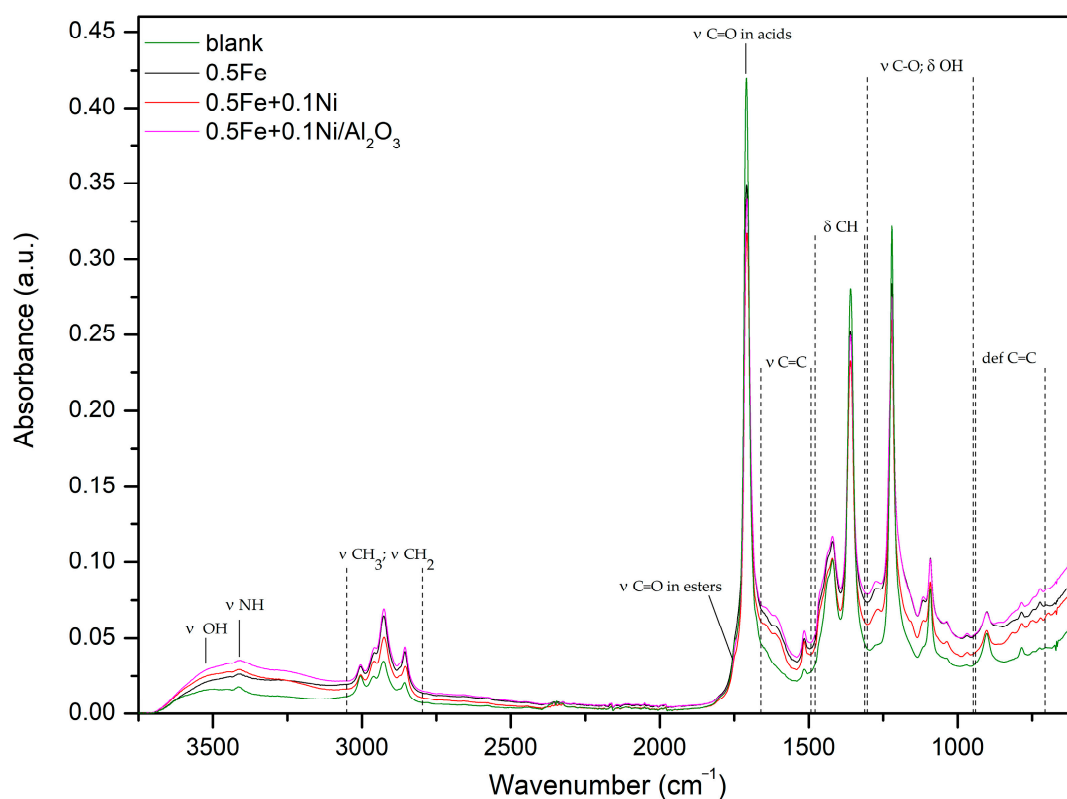


Figure 7. Infrared spectra of BM bio-crudes at 330 °C and for a residence time of 10 min.

More specifically, the bands at 3500 and 3416 cm^{-1} are characteristic of -OH stretching mode, which could be assigned to phenols, carboxylic acids or alcohols, and of -NH groups, respectively. Furthermore, the presence of these compounds is confirmed by the presence of the bands in the spectral range of 950–1300 cm^{-1} , which are ascribed to C–O stretching and -OH bending vibrations. The absorptions between 3000 and 2800 cm^{-1} (C–H stretching vibrations) are attributed to CH_3 and CH_2 stretching vibrations in the lipid acyl chains. The next band, centered at 1709 cm^{-1} , assigned to carbonyl groups (C=O stretching of the ester functional group), suggests the presence of oxygen compounds (aldehydes, ketones and carboxylic acids). This band is generally associated with free fatty acids [47], suggesting a high content of free fatty acids in the bio-crude, while the scarcely visible absorption at 1740 cm^{-1} is assigned to the C=O stretching vibration of the ester group in glycerides. Finally, unsaturated bonds (aromatic rings) could be ascribed to the low absorption stretching bands of C=C in the range 1660–1540 cm^{-1} and deformation vibrations at 700–950 cm^{-1} . The similarity of the infrared spectra recorded for all bio-oils reveals their similar qualitative features. However, as revealed by GC-MS analyses, the presence of the catalysts influences the quantitative composition of the bio-oils. In particular, the addition of Fe and Ni/ Al_2O_3 led to less intensive bands assigned to oxygenated compounds, mainly involving carbonyl groups and C–O bonds. These groups are less stable and break down to form simpler compounds. Moreover, the intensification of the bands corresponding to the stretching vibrations of the C=C in the aromatic compounds denotes more intense formation of phenols and its derivatives, which could originate from lignin or carbohydrates in the seed shell. Furthermore, an increasing absorbance intensity of the hydroxyl groups and methyl and methylene groups in the region 3700–2800 cm^{-1} could be ascribed to the re-arrangement of phenol derivatives.

4. Conclusions

The study of the influence of the operative condition and of the addition of catalysts on the HTL process is fundamental to maximize the quantity and quality of bio-oil production.

HTL tests were carried out with two different Ni-based catalysts (Ni metal and Ni supported on Al_2O_3) for the improvement of bio-crude yield and quality. The performances of the process were evaluated under different temperatures and reaction times to find the operative conditions that maximized the bio-crude yields. The chemical composition of the produced bio-crude was assessed by elemental analysis, FT-IR and GS-MS. According to the results, the increase of temperature promoted the formation of bio-crude, while the increase of the reaction time had a negative effect on bio-crude production; longer reaction times, in fact, favored condensation and repolymerization reactions, which contributed to the increase of gas and solid phases and to the decrease of both the oily and the water-soluble organic compound yields. The optimal operative conditions were a temperature of 330 °C and a reaction time of 10 min. The synergic effect between Fe, acting as hydrogen producer, and Ni, as catalyst, was demonstrated. Indeed, bio-crude yields of 57.18% and 48.23% for BS and BM, respectively, were obtained when the combination of Fe + Ni/ Al_2O_3 was used. The presence of the catalyst enhanced the quality of the bio-crude, leading to an increase of the H/C ratio of 1.56 and 1.31, respectively, and an ER value of $\approx 86.0\%$. Gas chromatography–mass spectrometry (GC-MS) and Fourier transform infrared spectroscopy (FT-IR) showed that the combined presence of Fe and Ni/ Al_2O_3 favored the hydrodeoxygenation of the fatty acids into long-chained hydrocarbons (C_{14} , C_{15} , C_{16} , C_{17}); indeed, an increase of $\approx 20\%$ was observed for both biomasses used. The results demonstrated that the catalytic HTL of *Brachichyton populneus* allows for valorization of the biomass components, producing a high-value liquid bio-crude that could be a perfect precursor to obtain bio-synthetic fuels and green chemical compounds.

Author Contributions: Conceptualization, B.d.C.; methodology, M.P.B. and M.D.; validation, M.P.B. and M.D.; investigation, I.E., M.P.B. and S.M.; resources, P.D.F.; data curation, M.P.B., M.D. and B.d.C.; writing—original draft preparation, I.E.; writing—review and editing, M.P.B., M.D. and B.d.C.; supervision, R.L.; funding acquisition, P.D.F. All authors have read and agreed to the published version of the manuscript.

Funding: This research received no external funding.

Data Availability Statement: The data presented in this study are available on request from the corresponding author.

Conflicts of Interest: The authors declare no conflict of interest.

References

1. Chen, W.T.; Qian, W.; Zhang, Y.; Mazur, Z.; Kuo, C.T.; Scheppe, K.; Schideman, L.C.; Sharma, B.K. Effect of ash on hydrothermal liquefaction of high-ash content algal biomass. *Algal Res.* **2017**, *25*, 297–306. [[CrossRef](#)]
2. Yerrayya, A.; Shree Vishnu, A.K.; Shreyas, S.; Chakravarthy, S.R.; Vinu, R. Hydrothermal Liquefaction of Rice Straw Using Methanol as Co-Solvent. *Energies* **2020**, *13*, 2618. [[CrossRef](#)]
3. Cao, M.; Long, C.; Sun, S.; Zhao, Y.; Luo, J.; Wu, D. Catalytic hydrothermal liquefaction of peanut shell for the production aromatic rich monomer compounds. *J. Energy Inst.* **2021**, *96*, 90–96. [[CrossRef](#)]
4. de Caprariis, B.; Bavasso, I.; Bracciale, M.P.; Damizia, M.; De Filippis, P.; Scarsella, M. Enhanced bio-crude yield and quality by reductive hydrothermal liquefaction of oak wood biomass: Effect of iron addition. *J. Anal. Appl. Pyrolysis* **2019**, *139*, 123–130. [[CrossRef](#)]
5. Brillman, D.W.F.; Drabik, N.; Wądrzyk, M. Hydrothermal co-liquefaction of microalgae, wood, and sugar beet pulp. *Biomass Convers. Biorefinery* **2017**, *7*, 445–454. [[CrossRef](#)]
6. Changi, S.M.; Faeth, J.L.; Mo, N.; Savage, P.E. Hydrothermal Reactions of Biomolecules Relevant for Microalgae Liquefaction. *Ind. Eng. Chem. Res.* **2015**, *54*, 11733–11758. [[CrossRef](#)]
7. Barrère-Mangote, C.; Roubaud, A.; Bouyssiere, B.; Maillard, J.; Hertzog, J.; Maitre, J.L.; Hubert-Roux, M.; Sassi, J.F.; Afonso, C.; Giusti, P. Study of biocrudes obtained via hydrothermal liquefaction (Htl) of wild alga consortium under different conditions. *Processes* **2021**, *9*, 1494. [[CrossRef](#)]
8. Leng, L.; Leng, S.; Chen, J.; Yuan, X.; Li, J.; Li, K.; Wang, Y.; Zhou, W. The migration and transformation behavior of heavy metals during co-liquefaction of municipal sewage sludge and lignocellulosic biomass. *Bioresour. Technol.* **2018**, *259*, 156–163. [[CrossRef](#)]
9. Biswas, B.; Bisht, Y.; Kumar, J.; Yenumala, S.R.; Bhaskar, T. Effects of temperature and solvent on hydrothermal liquefaction of the corncob for production of phenolic monomers. *Biomass Convers. Biorefinery* **2022**, *12*, 91–101. [[CrossRef](#)]

10. Carpio, R.B.; Zhang, Y.; Kuo, C.T.; Chen, W.T.; Schideman, L.C.; de Leon, R. Effects of reaction temperature and reaction time on the hydrothermal liquefaction of demineralized wastewater algal biomass. *Bioresour. Technol. Rep.* **2021**, *14*, 100679. [[CrossRef](#)]
11. Scarsella, M.; de Caprariis, B.; Damizia, M.; De Filippis, P. Heterogeneous catalysts for hydrothermal liquefaction of lignocellulosic biomass: A review. *Biomass Bioenergy* **2020**, *140*, 105662. [[CrossRef](#)]
12. Prasakti, L.; Rochmadi, R.; Budiman, A. The Effect of Biomass-Water Ratio on Bio-crude Oil Production from *Botryococcus braunii* using Hydrothermal Liquefaction Process. *J. Rekayasa Proses* **2019**, *13*, 132–138. [[CrossRef](#)]
13. Haarlemmer, G.; Guizani, C.; Anouti, S.; Déniel, M.; Roubaud, A.; Valin, S. Analysis and comparison of bio-oils obtained by hydrothermal liquefaction and fast pyrolysis of beech wood. *Fuel* **2016**, *174*, 180–188. [[CrossRef](#)]
14. Qian, L.; Zhao, B.; Wang, H.; Bao, G.; Hu, Y.; Charles Xu, C.; Long, H. Valorization of the spent catalyst from flue gas denitrogenation by improving bio-oil production from hydrothermal liquefaction of pinewood sawdust. *Fuel* **2022**, *312*, 122804. [[CrossRef](#)]
15. Nagappan, S.; Bhosale, R.R.; Nguyen, D.D.; Chi, N.T.L.; Ponnusamy, V.K.; Woong, C.S.; Kumar, G. Catalytic hydrothermal liquefaction of biomass into bio-oils and other value-added products—A review. *Fuel* **2021**, *285*, 119053. [[CrossRef](#)]
16. Sharma, N.; Jaiswal, K.K.; Kumar, V.; Vlaskin, M.S.; Nanda, M.; Rautela, I.; Tomar, M.S.; Ahmad, W. Effect of catalyst and temperature on the quality and productivity of HTL bio-oil from microalgae: A review. *Renew. Energy* **2021**, *174*, 810–822. [[CrossRef](#)]
17. Mukundan, S.; Xuan, J.; Dann, S.E.; Wagner, J.L. Highly active and magnetically recoverable heterogeneous catalyst for hydrothermal liquefaction of biomass into high quality bio-oil. *Bioresour. Technol.* **2023**, *369*, 128479. [[CrossRef](#)]
18. Nguyen, S.T.; Le, T.M.; Nguyen, H. Van Iron-catalyzed fast hydrothermal liquefaction of *Cladophora socialis* macroalgae into high quality fuel precursor. *Bioresour. Technol.* **2021**, *337*, 125445. [[CrossRef](#)]
19. de Caprariis, B.; Scarsella, M.; Bavasso, I.; Bracciale, M.P.; Tai, L.; De Filippis, P. Effect of Ni, Zn and Fe on hydrothermal liquefaction of cellulose: Impact on bio-crude yield and composition. *J. Anal. Appl. Pyrolysis* **2021**, *157*, 105225. [[CrossRef](#)]
20. Biswas, B.; Kumar, A.; Kaur, R.; Krishna, B.B.; Bhaskar, T. Catalytic hydrothermal liquefaction of alkali lignin over activated bio-char supported bimetallic catalyst. *Bioresour. Technol.* **2021**, *337*, 125439. [[CrossRef](#)]
21. Durak, H.; Genel, S. Catalytic hydrothermal liquefaction of *lactuca scariola* with a heterogeneous catalyst: The investigation of temperature, reaction time and synergistic effect of catalysts. *Bioresour. Technol.* **2020**, *309*, 123375. [[CrossRef](#)] [[PubMed](#)]
22. Zhao, B.; Li, H.; Wang, H.; Hu, Y.; Gao, J.; Zhao, G.; Ray, M.B.; Xu, C.C. Synergistic effects of metallic Fe and other homogeneous/heterogeneous catalysts in hydrothermal liquefaction of woody biomass. *Renew. Energy* **2021**, *176*, 543–554. [[CrossRef](#)]
23. Ding, Y.J.; Zhao, C.X.; Liu, Z.C. Catalytic hydrothermal liquefaction of rice straw for production of monomers phenol over metal supported mesoporous catalyst. *Bioresour. Technol.* **2019**, *294*, 122097. [[CrossRef](#)] [[PubMed](#)]
24. Saber, M.; Golzary, A.; Hosseinpour, M.; Takahashi, F.; Yoshikawa, K. Catalytic hydrothermal liquefaction of microalgae using nanocatalyst. *Appl. Energy* **2016**, *183*, 566–576. [[CrossRef](#)]
25. Kalnes, T.N.; Koers, K.P.; Marker, T.; Shonnard, D.R. A techno-economic and environmental life cycle comparison of green diesel to biodiesel and syndiesel. *Environ. Prog. Sustain. Energy* **2009**, *28*, 111–120. [[CrossRef](#)]
26. Kim, D.; Vardon, D.R.; Murali, D.; Sharma, B.K.; Strathmann, T.J. Valorization of Waste Lipids through Hydrothermal Catalytic Conversion to Liquid Hydrocarbon Fuels with in Situ Hydrogen Production. *ACS Sustain. Chem. Eng.* **2016**, *4*, 1775–1784. [[CrossRef](#)]
27. Mishra, V.K.; Goswami, R. A review of production, properties and advantages of biodiesel. *Biofuels* **2017**, *9*, 273–289. [[CrossRef](#)]
28. Di Vito Nolfi, G.; Gallucci, K.; Rossi, L. Green Diesel Production by Catalytic Hydrodeoxygenation of Vegetables Oils. *Int. J. Environ. Res. Public Health* **2021**, *18*, 13041. [[CrossRef](#)]
29. Vardon, D.R.; Sharma, B.K.; Jaramillo, H.; Kim, D.; Choe, J.K.; Ciesielski, P.N.; Strathmann, T.J. Hydrothermal catalytic processing of saturated and unsaturated fatty acids to hydrocarbons with glycerol for in situ hydrogen production. *Green Chem.* **2014**, *16*, 1507–1520. [[CrossRef](#)]
30. Liu, X.; Yang, M.; Deng, Z.; Dasgupta, A.; Guo, Y. Hydrothermal hydrodeoxygenation of palmitic acid over Pt/C catalyst: Mechanism and kinetic modeling. *Chem. Eng. J.* **2021**, *407*, 126332. [[CrossRef](#)]
31. Cheah, K.W.; Taylor, M.J.; Osatiashiani, A.; Beaumont, S.K.; Nowakowski, D.J.; Yusup, S.; Bridgwater, A.V.; Kyriakou, G. Monometallic and bimetallic catalysts based on Pd, Cu and Ni for hydrogen transfer deoxygenation of a prototypical fatty acid to diesel range hydrocarbons. *Catal. Today* **2020**, *355*, 882–892. [[CrossRef](#)]
32. Dawood, S.; Koyande, A.K.; Ahmad, M.; Mubashir, M.; Asif, S.; Klemeš, J.J.; Bokhari, A.; Saqib, S.; Lee, M.; Qyyum, M.A.; et al. Synthesis of biodiesel from non-edible (*Brachycthon populneus*) oil in the presence of nickel oxide nanocatalyst: Parametric and optimisation studies. *Chemosphere* **2021**, *278*, 130469. [[CrossRef](#)]
33. Ezeagu, I.E.; Petzke, J.K.; Metges, C.C.; Akinsoyinu, A.O.; Ologhobo, A.D. Seed protein contents and nitrogen-to-protein conversion factors for some uncultivated tropical plant seeds. *Food Chem.* **2002**, *78*, 105–109. [[CrossRef](#)]
34. Hamidi, R.; Tai, L.; Paglia, L.; Scarsella, M.; Damizia, M.; De Filippis, P.; Musivand, S.; de Caprariis, B. Hydrotreating of oak wood bio-crude using heterogeneous hydrogen producer over Y zeolite catalyst synthesized from rice husk. *Energy Convers. Manag.* **2022**, *255*, 115348. [[CrossRef](#)]
35. Tai, L.; Hamidi, R.; Paglia, L.; De Filippis, P.; Scarsella, M.; de Caprariis, B. Lignin-enriched waste hydrothermal liquefaction with ZVMs and metal-supported Al₂O₃ catalyst. *Biomass Bioenergy* **2022**, *165*, 106594. [[CrossRef](#)]

36. García, R.; Pizarro, C.; Lavín, A.G.; Bueno, J.L. Biomass proximate analysis using thermogravimetry. *Bioresour. Technol.* **2013**, *139*, 1–4. [[CrossRef](#)]
37. Dimitriadis, A.; Bezergianni, S. Hydrothermal liquefaction of various biomass and waste feedstocks for biocrude production: A state of the art review. *Renew. Sustain. Energy Rev.* **2017**, *68*, 113–125. [[CrossRef](#)]
38. Dandamudi, K.P.R.; Muppaneni, T.; Markovski, J.S.; Lammers, P.; Deng, S. Hydrothermal liquefaction of green microalga *Kirchneriella* sp. under sub- and super-critical water conditions. *Biomass Bioenergy* **2019**, *120*, 224–228. [[CrossRef](#)]
39. Chan, Y.H.; Yusup, S.; Quitain, A.T.; Uemura, Y.; Sasaki, M. Bio-oil production from oil palm biomass via subcritical and supercritical hydrothermal liquefaction. *J. Supercrit. Fluids* **2014**, *95*, 407–412. [[CrossRef](#)]
40. Aljabri, H.; Das, P.; Khan, S.; AbdulQuadir, M.; Thaher, M.; Hawari, A.H.; Al-Shamary, N.M. A study to investigate the energy recovery potential from different macromolecules of a low-lipid marine *Tetraselmis* sp. biomass through HTL process. *Renew. Energy* **2022**, *189*, 78–89. [[CrossRef](#)]
41. Hao, B.; Xu, D.; Jiang, G.; Sabri, T.A.; Jing, Z.; Guo, Y. Chemical reactions in the hydrothermal liquefaction of biomass and in the catalytic hydrogenation upgrading of biocrude. *Green Chem.* **2021**, *23*, 1562–1583. [[CrossRef](#)]
42. Li, D.; Chen, L.; Xu, D.; Zhang, X.; Ye, N.; Chen, F.; Chen, S. Preparation and characteristics of bio-oil from the marine brown alga *Sargassum patens* C. Agardh. *Bioresour. Technol.* **2012**, *104*, 737–742. [[CrossRef](#)] [[PubMed](#)]
43. Sugano, M.; Takagi, H.; Hirano, K.; Mashimo, K. Hydrothermal liquefaction of plantation biomass with two kinds of wastewater from paper industry. *J. Mater. Sci.* **2008**, *43*, 2476–2486. [[CrossRef](#)]
44. Tai, L.; de Caprariis, B.; Scarsella, M.; De Filippis, P.; Marra, F. Improved Quality Bio-Crude from Hydrothermal Liquefaction of Oak Wood Assisted by Zero-Valent Metals. *Energy Fuels* **2021**, *35*, 10023–10034. [[CrossRef](#)]
45. Zhang, B.; Lin, Q.; Zhang, Q.; Wu, K.; Pu, W.; Yang, M.; Wu, Y. Catalytic hydrothermal liquefaction of *Euglena* sp. microalgae over zeolite catalysts for the production of bio-oil. *RSC Adv.* **2017**, *7*, 8944–8951. [[CrossRef](#)]
46. Kim, K.H.; Brown, R.C.; Kieffer, M.; Bai, X. Hydrogen-donor-assisted solvent liquefaction of lignin to short-chain alkylphenols using a micro reactor/gas chromatography system. *Energy Fuels* **2014**, *28*, 6429–6437. [[CrossRef](#)]
47. Dong, X.; Li, Q.; Sun, D.; Chen, X.; Yu, X. Direct FTIR Analysis of Free Fatty Acids in Edible Oils Using Disposable Polyethylene Films. *Food Anal. Methods* **2015**, *8*, 857–863. [[CrossRef](#)]

Disclaimer/Publisher’s Note: The statements, opinions and data contained in all publications are solely those of the individual author(s) and contributor(s) and not of MDPI and/or the editor(s). MDPI and/or the editor(s) disclaim responsibility for any injury to people or property resulting from any ideas, methods, instructions or products referred to in the content.